Enhanced bio-barcode immunoassay using droplet digital PCR for multiplex detection of organophosphate pesticides

Xueyan Cui[a], A. M. Abd El-Aty[b,c,d], Chan Zhang[a], Lingyuan Xu[a], Haijin Liu[e], Huiyan Jia[f], Yuanshang Wang[a], Zhen Cao[a], J.-Pablo Salvador[g,h], Yongxin She[a], Fen Jin[a], Jing Wang[a,*], Maojun Jin[a,*], Bruce D. Hammock[i]

[a] *Institute of Quality Standard and Testing Technology for Agro-Products, Chinese Academy of Agricultural Science, Beijing 100081, P. R. China*

[b]*State Key Laboratory of Biobased Material and Green Papermaking, College of Food Science and Engineering, Qilu University of Technology, Shandong Academy of Science, Jinan 250353, China*

[c]*Department of Pharmacology, Faculty of Veterinary Medicine, Cairo University, 12211-Giza, Egypt*

[d]*Department of Medical Pharmacology, Medical Faculty, Ataturk University, Erzurum 25240, Turkey*

[e]*Inspection and Testing Center of Agricultural and Livestock Products of Tibet, Lhasa 850000, P.R. China*

[f] *Ningbo Academy of Agricultural Sciences, Ningbo, Zhengjiang 315040, P.R. China*

[g]*Nanobiotechnology for Diagnostics group. Instituto de Química Avanzada de Cataluña, IQAC-CSIC, C/ Jordi Girona 18-26, 08034, Barcelona*

[h]*CIBER de Bioingeniería, Biomateriales y Nanomedicina (CIBER-BBN), Av. Monforte de Lemos, 3-5. Pavillion 11. Floor 0 28029 Madrid, Spain*

[i]*Department of Entomology & Nematology and the UC Davis Comprehensive Cancer Center, University of California, Davis, CA, 95616, USA*

25 *** Corresponding authors:**

26 **Tel.**: +86-10-8210-6568; **E-mail**: wangjing05@caas.cn (J. Wang)

27 **Tel.**: +86-10-8210-6570. **E-mail**: jinmaojun@caas.cn (M. J. Jin)

28

ABSTRACT: A bio-barcode immunoassay based on droplet-digital PCR (ddPCR) was developed to simultaneously quantify triazophos, parathion, and chlorpyrifos in apple, cucumber, cabbage, and pear. Three gold nanoparticle (AuNP) probes and magnetic nanoparticle (MNP) probes were prepared, binding through their antibodies with the three pesticides in the same tube. Three groups of primers, probes, templates, and three antibodies were designed to ensure the specificity of the method. Under the optimal conditions, the detection limits (expressed as IC_{10}) of triazophos, parathion, and chlorpyrifos were 0.22, 0.45, and 4.49 ng mL^{-1}, respectively. The linear ranges were 0.01-20, 0.1–100, and 0.1–500 ng mL^{-1}, and the correlation coefficients (R^2) were 0.9661, 0.9834, and 0.9612, respectively. The recoveries and relative standard deviations (RSDs) were in the ranges of 75.5–98.9% and 8.3–16.7%. This study provides the first insights into the ddPCR for the determination of organophosphate pesticides. It also laid the foundation for high-throughput detection of other small molecules.

KEYWORDS: Gold nanoparticles; Magnetic nanoparticles; Oligonucleotides; ddPCR; Organophosphate pesticides

INTRODUCTION

Organophosphate pesticides (OPs), a class of organic compounds containing phosphorus, are used to increase crop yields and control diseases and pests. Multiple pesticides are often found together in agricultural products, soil, water[1,2], which present dangers to humans and ecological systems[3,4]. Compared to the simultaneous determination of various analytes chromatographically, detection by different single-residue methods has the disadvantage of time-consuming, repetitive operations. On the contrary, an approach that can concurrently detect multiple pesticides in a single well or tube would lead to an easy, fast, and inexpensive procedure[5-8]. Therefore, current research on multi-residue analysis is of great importance. There are two main methods for multi-residue detection of pesticides and other small molecule contaminants. The first category is preparing antibodies that can recognize one class of pesticides by a universal hapten. The second category is through various single haptens and various specific monoclonal antibodies for multiplex residue detection. In comparison, the pitfall of the first approach is that the method detects the concentration level of a class of pesticides; however, it does not explicitly determine the concentration level of a given pesticide. Notably, the second type is widely used at this stage due to its reasonable specificity and ease of handling.

Digital PCR is a new technology that enables absolute quantification[10]. In 1992, Higuchi et al. [11,12] proposed three fundamental principles that laid the foundation for the development of digital PCR; then, in 1999, Bert Vogelstein and Ken Kinzler officially named it digital PCR (dPCR)[13]. In 2006, Fluidigm produced the first

commercially available chip-based dPCR, whereas, in 2011, Bio-Rad produced the first commercially available ddPCR. At last, Stilla made the first commercially available Crystal digital PCR in 2016. The ddPCR can detect a variety of viruses[14-17], pathogenic bacteria[18-21], heavy metals[22,23], and transgenes[24-27]. In this context, our group first applied it for the detection of pesticide contaminants[28]. Before the traditional PCR amplification, the reaction systems containing nucleic acid molecules are divided into thousands of microdroplets. Each microdroplet contains either zero or one to several nucleic acid strands to be detected. After PCR amplification, each microdroplet can be examined one by one, and microdroplets with fluorescence signals are interpreted as "1", whereas those without any fluorescent signal are interpreted as "0". The Poisson distribution principle can reliably obtain a copy of the target molecule and the number or proportion of positive microdroplets [29]. Compared with the traditional Real-time Quantitative PCR (qPCR), it is more sensitive, stable, and practical.

Herein, we present a digital PCR-based bio-barcode immunoassay for the simultaneous detection of three OPs, triazophos, parathion, and chlorpyrifos. Three AuNP probes were designed by attaching antibodies and corresponding double chain DNAs to colloidal gold. Three MNP probes were prepared by attaching ovalbumin-haptens (OVA-haptens) to magnetic nanoparticles. The structures of triazophos, parathion, and chlorpyrifos haptens are shown in Figure 1. A mixture of AuNP probes was inserted into the centrifuge tube, followed by a mix of MNP probes and mixed standards of the three pesticides for magnetic separation after immunocompetitive

reactions. The three bio-barcode DNA strands under dissociation were subjected to multi-residue detection on ddPCR.

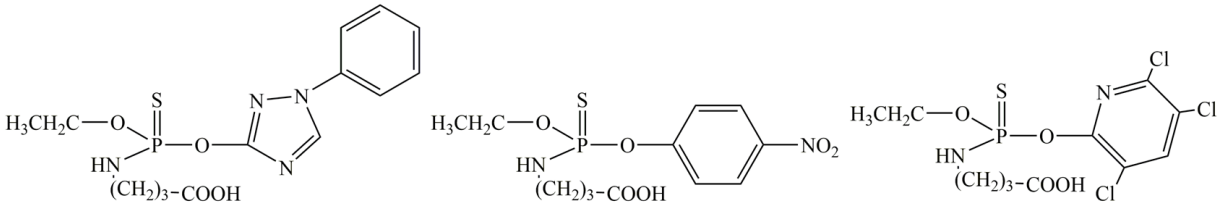

Figure 1. Structure of triazophos, parathion, and chlorpyrifos haptens used for coating antigens.

Materials and methods

Materials and oligonucleotides

Triazophos, parathion, and chlorpyrifos standards (purity, 98%), bovine serum albumin (BSA), polyethylene glycol 20000 (PEG20000), Tris EDTA (TE) buffer (pH7.4), ethylsulfonic acid (MES), 1-(3-dimethylaminopropyl)-3-ethylcarbodiimide (EDC), N-hydroxysuccinimide (NHS), chlorogold acid ($HAuCl_4 \cdot 3H_2O$), and trisodium citrate were acquired from Sigma Aldrich (St. Louis, MO, USA). The monoclonal antibodies against triazophos, parathion, and chlorpyrifos were provided by the Pesticide and Environmental Toxicology Group of Zhejiang University (Hangzhou, China). N-propyl ethylenediamine (PSA) and octadecyltrimethoxysilane (C_{18}) were secured from Tianjin Bona Agela Technology Company (Tianjin, China). Thermo Fisher Scientific Company (Waltham, MA, USA) supplied magnetic nanoparticles with a carboxyl group and chromatographic grade acetonitrile and methanol. Potassium carbonate (K_2CO_3), sodium chloride (NaCl), and analytical grade organic solvents were purchased from Beijing Chemical Industry Group Co.,

Ltd. (Beijing, China). Droplet forming oil, droplet analysis oil, and ddPCR premix were purchased from Bio-Rad company (Hercules, CA, USA). qPCR premix was bought from Takara company (Tokyo, Japan). All the designed sequences are shown in Table 1. The designed sequences were synthesized by Shanghai Biotechnology Corporation (Shanghai, China).

The following buffers were prepared and used throughout the experimental work: (1) 0.01 mol L^{-1} phosphate-buffered solution (PBS, pH 7.4); (2) 3% BSA blocking solution: 30 mg BSA was weighed and dissolved in 1 mL 0.01 mol L^{-1} PBS (pH 7.4) (3) Washing buffer: 0.01 mol L^{-1} PBS (pH 7.4) and 0.05% Tween-20, 0.01 mol L^{-1}, MES buffer (pH 6.0); (4) Probe buffer: 0.01 mol L^{-1} PBS was used to dilute 3% BSA to 1% BSA and 30% PEG 20000 to 1%, respectively.

Table 1. List of oligonucleotide sequences used in this study.

Function	Sequence (5'–3')
The barcodes DNA-1	GAATCTGTGCGGCAATGTCATTAATACATTTAACGTGAGA ACGCGCCGTACCGATGCTGAGCAAGTCA
The thiolated DNA-1	HS(T)10TGACTTGCTCAGCATCGGTACGGCGCGTTCTCAC GTTAAATGTATTAATGACATTGCCGCACAGATTC
Forward primer -1	GAATCTGTGCGGCAATGTC
Reverse primer -1	TGACTTGCTCAGCATCGGT
Probe -1	FAM-ATTAATACATTTAACGTGAGAACGCGCC-BHQ1
The barcodes DNA-2	CTCTCGACGCAGTCACGAGCGTACGTCACGTAGCCTGCT AGCGAGCATACGATCTCGGTCGATGCCTG
The thiolated DNA-2	$HS(T)_{10}$CAGGCATCGACCGAGATCGTATGCTCGCTAGCAG

	GCTACGTGACGTACGCTCGTGACTGCGTCGAGAG
Forward primer -2	CTCTCGACGCAGTCACGAG
Reverse primer -2	CAGGCATCGACCGAGATCG
Probe -2	FAM- CGTACGTCACGTAGCCTGCTAGCGAGCA-BHQ1
The barcodes DNA-3	CAGCTCACCTGTAGCAGCTACGTGGCACCATGGATGTGC
	CGTCTGAGCAGAGACACGCTGCTACTGCA
The thiolated DNA-3	$HS(T)_{10}$TGCAGTAGCAGCGTGTCTCTGCTCAGACGGCACA
	TCCATGGTGCCACGTAGCTGCTACAGGTGAGCTG
Forward primer -3	CAGCTCACCTGTAGCAGCT
Reverse primer -3	TGCAGTAGCAGCGTGTCTC
Probe -3	FAM-ACGTGGCACCATGGATGTGCCGTCTGAG-BHQ1

FAM: carboxyfluorescein

BHQ: black hole quencher

Primers, probes, and templates design

Two additional sets of upstream and downstream primers, probes, and DNA sequences were designed according to the flowchart shown in Figure 2. The three designed DNA strands were paired for blast sequence alignment. If the results showed "Identities," the upstream and downstream primers, probes, and DNA sequences were re-modified according to the identity results until there was no identity among the three DNA sequences. The designed DNA sequences, primers, and probes were amplified on the qPCR instrument to determine whether the target sequences can be amplified. Sequences 1, 2, and 3 were assigned to triazophos, parathion, and chlorpyrifos, respectively, and sequence 1 was selected based on the previous

literature[28]. PCR amplified DNA sequences 1, 2, and 3 with probes and primers to determine the specificity of the three groups of sequences. The upstream and downstream primers, probes, and DNA sequences were redesigned if the specificity was not reasonable.

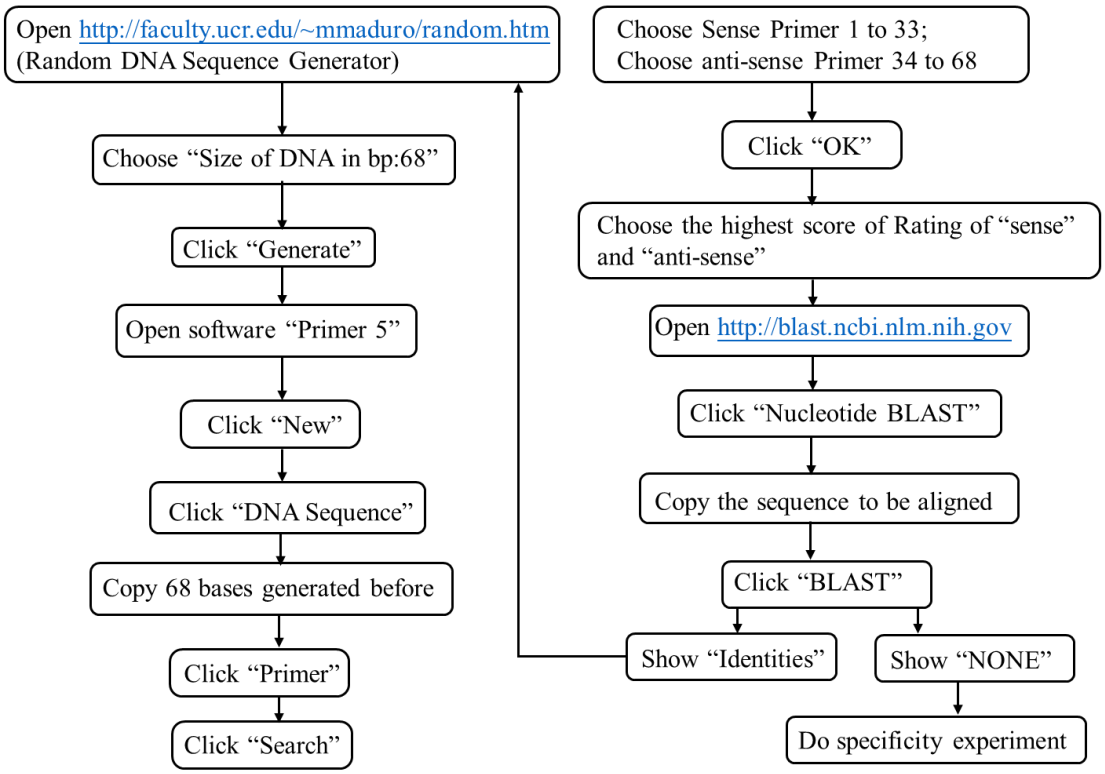

Figure 2. Flowchart of oligonucleotide design.

Preparation of three AuNP probes

The unsealed centrifuge tubes with thiolated DNA powder were centrifuged at 10000 rpm for 3 min. After centrifugation, a specific volume of TE buffer was added to stabilize the DNA according to the instructions, and the same volume as TE buffer of 20 mmol L^{-1} TCEP solution was added. The tubes were shaken at room temperature for more than 1 h for activation.

The specific procedure was based on our previous report[28]. Briefly, 15 μL of 0.2 mol L^{-1} K_2CO_3 solution was put into each of three glass bottles containing 1 mL

AuNP solution to adjust the pH between 9.0 and 9.5. After that, 4 μL triazophos antibody (4.53 mg L^{-1}), 8 μL parathion antibody (7.57 mg L^{-1}), and 16 μL chlorpyrifos antibody (10.2 mg L^{-1}) were added to the solution, blown with a gun, and left to mix for 1 h. Then, the pre-activated DNA solution was added to the AuNP solution containing antibodies, yielding a final concentration of 3 μmol L^{-1} with thiolated DNA kept in a refrigerator at 4 °C overnight. A 30% PEG solution was added to give a final concentration of 0.5%, followed by six additions of 0.1 mol L^{-1} PBS over 40 h to give a final concentration of 0.01 mol L^{-1}. Subsequently, 3% BSA was added to the solution to achieve a final concentration of 1% and incubated for 40 min. Next, the supernatant was discarded, and the solution was resuspended in a 500 μL probe buffer. Finally, the barcode DNA (a complementary strand of the thiolated DNA strand), which had been centrifuged in advance and added to TE buffer, was added to the above-stated probe buffer. The solution was left at room temperature for 4 h to achieve hybridization. The supernatant was discarded, and the solution was resuspended in 500 μL probe buffer and set aside at 4 °C.

Preparation of three MNP probes

Separately, 1 mL of MNPs solution was added to the three centrifuge tubes, MES buffer was added to each tube and vortexed for 5 s. The supernatant was separated and removed on a magnetic stand, and 1 mL MES buffer was then used to wash the magnetic beads three times. After that, 500 μL MES buffer, 500 μL of 10 mg mL^{-1} EDC, and 500 μL of 10 mg mL^{-1} NHS were mixed into the centrifuge tube with gentle shaking at ambient temperature for 30 min. The supernatant was manually

175 removed using a magnetic stand and rinsed four times with washing buffer followed
176 by adding 800 μg of 5 mg mL^{-1} triazophos-OVA, 800 μg of 10 mg mL^{-1} parathion-
177 OVA, and 800 μg of 7 mg mL^{-1} chlorpyrifos-OVA to three tubes. The mixtures were
178 placed at a constant temperature (37 °C) and humidity chamber for 16 h with gentle
179 shaking. Finally, 2% BSA was added to the centrifuge tubes and incubated at room
180 temperature for 40 min. The synthesized MNP probes were resuspended in 500 μL
181 probe buffer and stored at 4 °C pending use.

182 **Bio-barcode immunoassay based on ddPCR**

183 First, the three previously prepared AuNP and three MNP probes were diluted to
184 the corresponding multiples with 0.01 mol L^{-1} of PBS solution. A 50 μL diluted
185 mixture of the three AuNP probes solution was added into a centrifuge tube to which
186 20 μL of the corresponding MNP probes and 20 μL of a mix of triazophos, parathion,
187 and chlorpyrifos standards were added immediately. After mixing, the tube was
188 shaken for 15 min at 37 °C. After four rinses with 0.01 mol L^{-1} of PBS solution, 100
189 μL deionized water was added, and the tubes were kept at a constant temperature of
190 60 °C for 50 min. Finally, the supernatant was collected and measured by ddPCR. The
191 specific qPCR and ddPCR amplification systems are shown as following.

192 *qPCR amplification system*

193 (1) A 25 μL reaction system was prepared in a qPCR tube, and the blank wells are:

194 Probe qPCR Mix 12.5 μL

195 Upstream primer 1 μL

196 Downstream primer 1 μL

Probe 0.5 μL

Deionized water 10 μL

(2) A 25 μL reaction system was prepared in a qPCR tube, and the experimental wells are:

Probe qPCR Mix 12.5 μL

Upstream primer 1 μL

Downstream primer 1 μL

Probe 0.5 μL

Target sequence 2 μL

Deionized water 8 μL

(3) Conditions for qPCR amplification

Pre-denaturation 95 ℃, 10 min.

30 cycles { 95 °C, 30 s. / 59 ℃, 20 s. / 72 ℃, 10 s

Solubility curve: 60 ℃ to 95 ℃, 1 ℃ rise every 10 s.

ddPCR amplification system

(1) A 25 μL reaction system was prepared in DG8 cartridge, and the blank wells are:

ddPCR Supermix for probes 10 μL

Upstream primer 1 μL

Downstream primer 1 μL

Probe 0.5 μL

Deionized water 7.5 μL

(2) A 25 μL reaction system was prepared in DG8 cartridge, and the experimental wells are:

ddPCR Supermix for probes 10 μL

Upstream primer 1 μL

Downstream primer 1 μL

Probe 0.5 μL

Target sequence 2 μL

Deionized water 5.5 μL

(3) Conditions for ddPCR amplification

Pre-denaturation 95 °C for 5 min.

34 cycles { 94 ℃, 30 s.
58 °C, 40 s.

Extension 98 °C, 8 min.

Sample pretreatment

Samples of apple, cucumber, cabbage, and pear were procured from Wumei supermarket in Beijing. According to GB 2763-2019, the MRLs have been set at 50 μg kg^{-1} for triazophos in vegetables, 10 μg kg^{-1} for parathion in fruits and vegetables, and 50 μg kg^{-1} for chlorpyrifos in vegetables. Therefore, the mixed standard solutions of triazophos, parathion, and chlorpyrifos were spiked to each homogenized sample (10 g) as following: 5, 10, and 50 μg kg^{-1} for triazophos and parathion; and 10, 50, and 100 μg kg^{-1} for chlorpyrifos. The spiked samples were allowed to stand for at

least 2 h. After that, the samples were extracted with 10 mL acetonitrile vortexed for 5 min at 2500 rpm. Subsequently, 4 g $MgSO_4$ and 1 g NaCl were added to the mixture, shaken for 5 min at 2500 rpm, and then centrifuged at 6000 rpm for 6 min. Subsequently, 2 mL supernatant was aspirated to new tubes containing 100 mg PSA and 100 mg C_{18}. Similarly, the tubes were vortexed and centrifuged at 10,000 rpm for 6 min. Next, 100 μL supernatant was concentrated under nitrogen and resuspended in 2 mL of 5% methanol-0.01 mol L^{-1} PBS solution for the subsequent detection step with the developed method. The remaining supernatant was added to the injection vial for LC-MS/MS analysis, and the conditions of LC-MS/MS were referred to in Zhang et al. article [30].

RESULTS AND DISCUSSION

Primer and probe specificity

To verify the specificity of the probes and primers during PCR amplification, three sets of experiments were performed on the qPCR, and each set includes one control and 3 experimental groups. As shown in Figure 3A, DNA1-1 means barcodes DNA-1, forward primer-1, reverse primer-1, and probe-1 having a PCR amplification reaction in the same system. Likewise, DNA1-2 means barcodes DNA-1, forward primer-2, reverse primer-2, and probe-2 having a PCR amplification reaction in the same system. The blue line parallel to the abscissa has an intersection point with the qPCR curve; the abscissa value corresponding to the intersection point is the Ct value. The smaller the Ct value, the higher the amplification efficiency. The results showed that probes 2 and 3, primers 2 and 3 do not amplify barcodes DNA-1 efficiently.

According to Figures 3B and 3C, the primer-probe 1 can amplify barcodes DNA 2 and 3; however, the impact can be ignored as judged by the Ct value of DNA2-2 and DNA3-3 curves. The PCR amplification reactions of the unpaired primers, probes, and DNA sequences in each group of experiments had similar Ct values to PCR amplification reactions of no template control (NTC) wells, indicating high specificity of the primers and probe sets. PCR amplification reactions can usually occur without cross-reactivity.

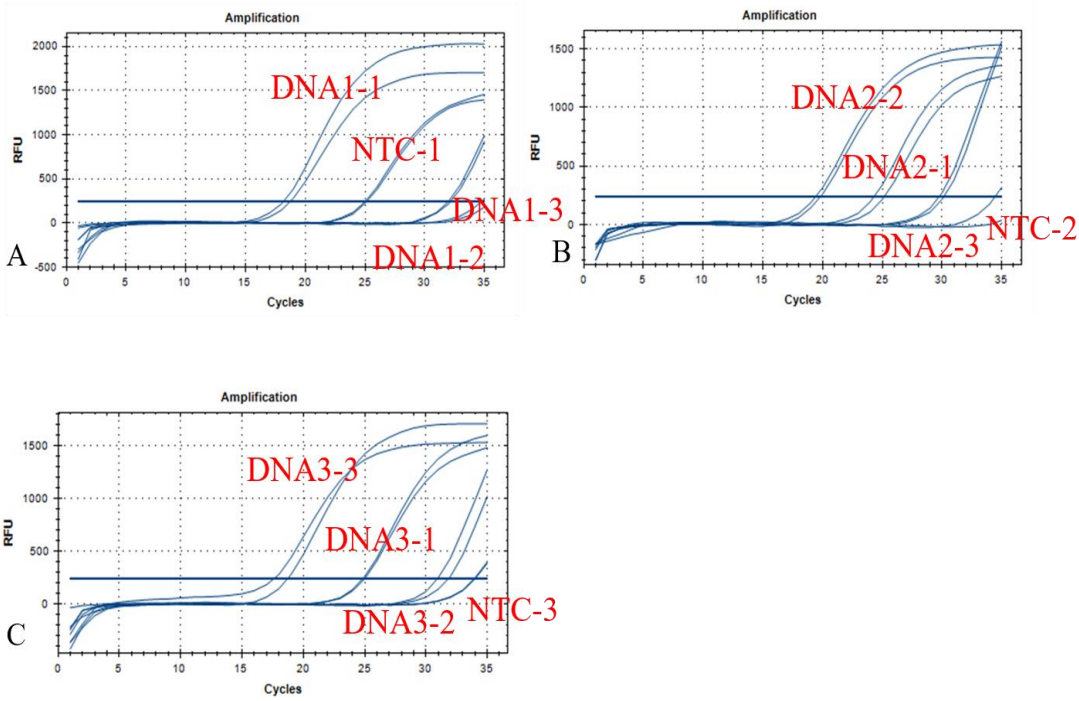

Figure 3. Cross-reactions between primers, probes, and barcodes DNA-1 (A), barcodes DNA-2 (B), and barcodes DNA-3 (C).

Optimization of ddPCR detection system

Optimization of annealing temperature

The optimization of annealing temperature has a crucial impact on PCR amplification. If the annealing temperature is too low, it will allow the primer and non-target template combination to result in non-specific amplification. At variance, it

is not conducive to the template for PCR amplification by the high annealing temperature. The annealing temperature is generally chosen to be approximately 5 °C higher than the Tm value. The temperature gradient of 65, 64.5, 63.3, 61.4, 59, 57, 55.7, and 55 °C was set for PCR amplification. As shown in Figure 4A, the optimal annealing temperature of the parathion primer and template was 59 °C. From Figure 4B, DNA sequence 3 corresponding to chlorpyrifos has no PCR amplification at 65, 64.5, and 63.3 °C. The optimal annealing temperature of DNA strand 3 was set at 57 °C, due to the efficient separation of positive and negative microdroplets. Our previous literature[28] reported the optimal annealing temperature of DNA strand 1 was 58 °C. Considering the optimal annealing temperature of DNA strands 1, 2, and 3 simultaneously, 58 °C has been chosen as the optimal one.

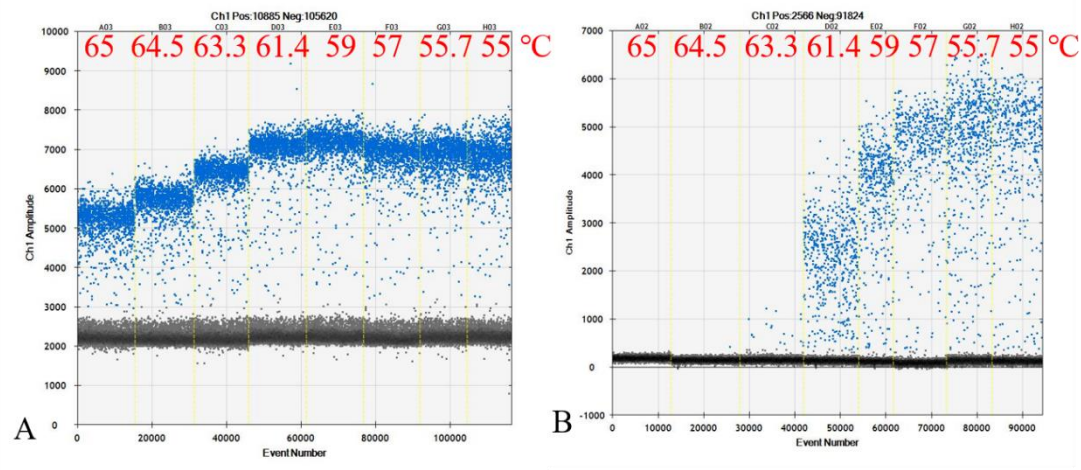

Figure 4. Optimization of annealing temperature for parathion (A) and chlorpyrifos (B).

Optimizing primer and probe concentrations

Probe and primer concentrations may have an impact on PCR amplification. If the probe and primer concentrations are not appropriate, it may cause poor separation

of negative and positive microdroplets or affect the amplification of the target sequence. Our previous literature[28] reported the optimal probe and primer concentrations of DNA strand 1 were 125 and 250 nmol L^{-1}. As shown the red numbers in figure 5, the primer and probe concentrations of DNA strands 2 and 3 were selected as 400 and 200 nmol L^{-1}, 240 and 120 nmol L^{-1}, and 80 and 40 nmol L^{-1}. It can be seen from the following two graphs that the separation of negative and positive microdroplets tends to be more and more efficient as the concentration of the probe and primer increases; however, the number of amplified target sequences is decreasing. Considering the two factors, 400 nmol L^{-1} and 200 nmol L^{-1} were selected to ensure the impact of PCR amplification.

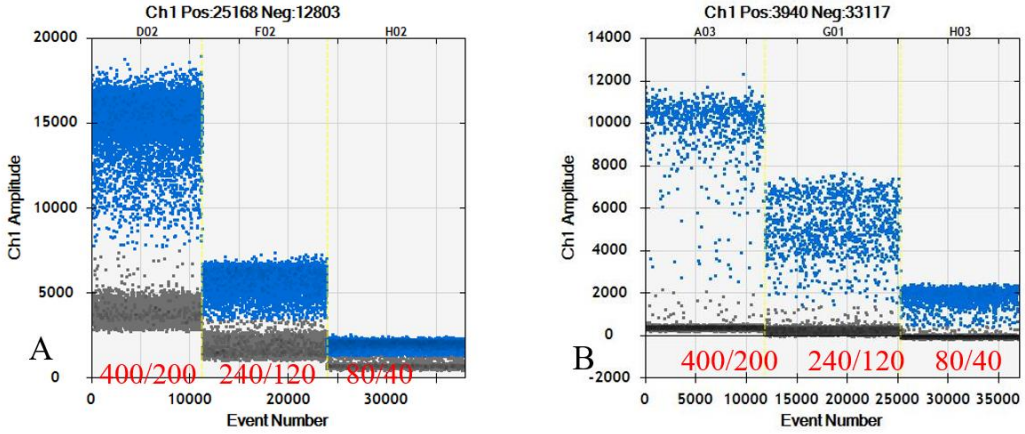

Figure 5. Optimization of primer and probe concentration for parathion (A) and chlorpyrifos (B).

Optimization of antibodies and oligonucleotides concentration for parathion and chlorpyrifos

The concentrations of antibodies and oligonucleotides play a key role in the stability of AuNP probes and method sensitivity. By adding antibodies at a volume of

4, 8, 16, and 32 μL, the concentration of antibodies was 30.3, 60.6, 121.2, and 242.2 mg/L (for parathion), and 25.2, 50.5, 101.0, and 202 mg/L (for chlorpyrifos), respectively. The amounts of oligonucleotides to AuNPs were added at molar ratios of 200:1, 300:1, 400:1, and 500:1, respectively. The corresponding concentration of oligonucleotides were 2, 3, 4, and 5 μmol L^{-1}. The rest of the conditions were kept consistent, and experiments were performed at a pesticide concentration of 0.5 μg L^{-1}; the inhibition rate was calculated under each condition. Similarly, the optimal volume of antibodies and the optimal oligonucleotides for triazophos were based on the previous report[28]. The results can be seen in Figure 6; the optimal volume of antibodies was 8 and 16 μL for parathion chlorpyrifos, respectively. The optimal two types of oligonucleotides were all set at 300:1.

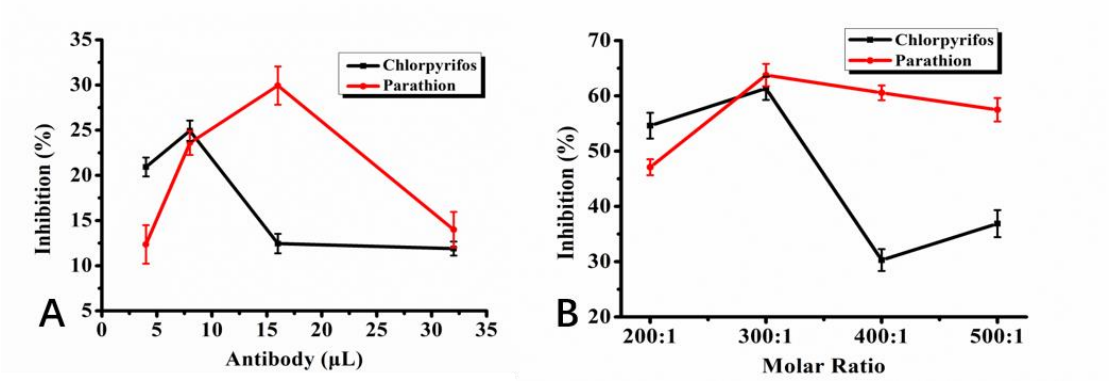

Figure 6. Optimization of antibody (A) and dsDNA (B) concentrations for parathion and chlorpyrifos.

Specificity of AuNP probes for triazophos, parathion, and chlorpyrifos

Antibody-specific recognition of pesticides is the premise to ensure the accuracy of the results. Three experiments were conducted to verify the specificity of triazophos, parathion, and chlorpyrifos mixed AuNP probes. In each experiment group,

a single MNP probe reacted with a single AuNP probe, a mixed MNP probe reacted with a single AuNP probe, and a single MNP probe responded with a mixed AuNP probe (Figure 7A). Where samples 1, 2, 3, and 4 represent reactions of chlorpyrifos, samples 5, 6, 7, and 8 represent reactions of parathion, and samples 9, 10, 11, and 12 represent reactions for triazophos. AuNP probes of triazophos, parathion, and chlorpyrifos were diluted 20-fold. MNP probes for triazophos, parathion, and chlorpyrifos were diluted 80-fold, 40-fold, and 20-fold, respectively, and pesticide concentrations were maintained at 5 ng ml^{-1} for competitive reaction. As presented in Figure 7B, the concentration value corresponding to the response of chlorpyrifos AuNP probe with mixed MNP probes was slightly higher than that of a single AuNP probe and single MNP probe. Similarly, the concentration value of chlorpyrifos (corresponding to the reaction of mixed MNP probes and mixed AuNP probes) was higher than that of chlorpyrifos under a single reaction. We can imply that chlorpyrifos AuNP probe might have a recognition effect on triazophos and parathion MNP probes; however, the differences are within the acceptable range and can be used to detect multiple pesticide residues.

A

Sample 1, 5, 9	Sample 2, 6, 10	Sample 3, 7, 11	Sample 4, 8, 12
Single MNP probes + single AuPNs probes	Single MNP probes + mixed AuPNs probes	Mixed MNP probes + single AuPNs probes	Mixed MNP probes + mixed AuPNs probes

B

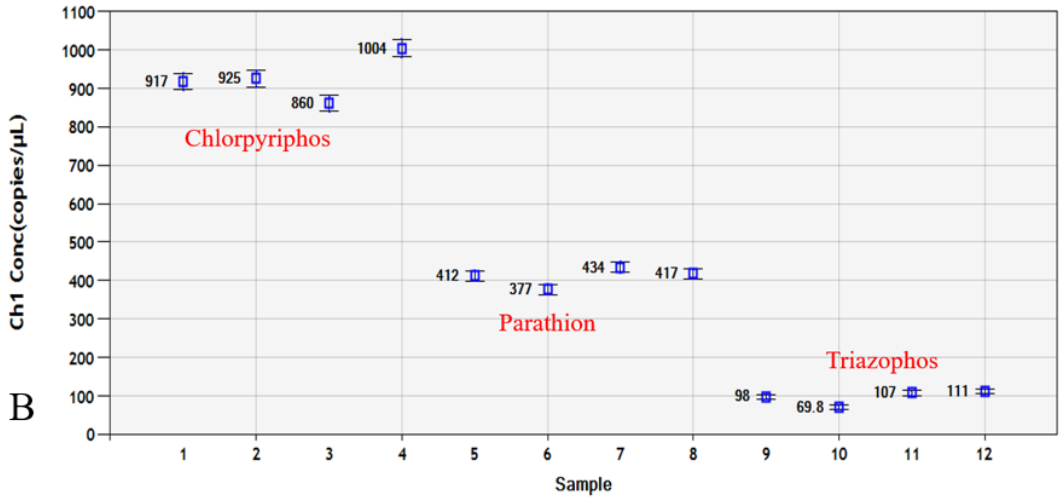

Figure 7. (A) Schematic representation for cross-reactivity of the three AuNP probes. (B) The result of cross-reactions between AuNP and MNP probes of triazophos, parathion, and chlorpyrifos.

Establishment of a ddPCR-based bio-barcode immunoassay for multi-residue detection of OPs

Optimization of working concentration of antigens and antibodies

To establish a stable and sensitive bio-barcode immunoassay based on a ddPCR, it is necessary to optimize the working concentration of antigens (MNP probes) and antibodies (AuNP probes) for triazophos, parathion, and chlorpyrifos. The MNP probes were diluted by 20-, 40-, and 80-fold, and the AuNP probes were diluted by 10, 20, and 40-fold, respectively. The concentration of the mixed standard solution of pesticides was 0.5 ng mL^{-1}. The immune reactions of different dilution multiples of MNP probes and AuNP probes were carried out with and without pesticides, and inhibition rates were calculated. According to the value of inhibition rate, the optimal

dilution ratio of antibodies and antigens was determined. The results are shown in Table 2. It was evident from the results that the optimal AuNP and MNP probes dilution multiples were 20 and 80 for triazophos, 20 and 40 for parathion, and 20 and 20 for chlorpyrifos.

Table 2. Optimization of the working concentration of antigen and antibody.

Pesticides	Dilution multiples of AuNP probe (mg L^{-1})	Dilution multiples of MNP probe (mg L^{-1})	Inhibition (%)
Triazophos	×10	×20	54.3
		×40	33.4
		×80	24.6
	×20	×20	59.9
		×40	54.6
		×80	61.2
	×40	×20	42.1
		×40	31.6
		×80	29.4
Parathion	×10	×20	46.9
		×40	37.7
		×80	19.0
	×20	×20	49.2
		×40	55.9
		×80	30.8
	×40	×20	28.5
		×40	20.5
		×80	28.5
Chlorpyrifos	×10	×20	41.1
		×40	12.6
		×80	8.87
	×20	×20	60.0
		×40	42.5
		×80	19.5
	×40	×20	51.9
		×40	43.9
		×80	29.3

Establishment of the standard curve

After optimization of the experimental conditions, the standard curves were constructed. The mixed standards of the three pesticides were diluted with 5%

methanol-0.01 mol L^{-1} PBS solution into a series of gradients in the range of 0.01-1000 ng mL^{-1}. The half-maximal inhibitory concentration (IC_{50}) indicates the concentration of pesticide required when the inhibition rate reaches 50%. Similarly, IC_{10} indicates the concentration of pesticide required when the inhibition rate reaches 10%, representing the method's detection limit in this experiment. The values of IC_{50} and IC_{10} for triazophos, parathion, and chlorpyrifos were 0.22, 0.45, and 4.49 ng mL^{-1}; 0.004, 0.007, and 0.121 ng mL^{-1}. Good linearity in the range of 0.01-20 ng mL^{-1}, 0.1-100 ng mL^{-1}, and 0.1-500 ng mL^{-1} with linear correlation equation of y = 22.45x + 64.69 (R^2=0.9661), y = 22.55x + 57.74 (R^2=0.9834), and y = 25.44x + 33.39 (R^2=0.9612) have been shown for triazophos, parathion, and chlorpyrifos, respectively (Table 4 and Figure 8). In summary, the ddPCR-based bio-barcode immunoassay reported here displayed high sensitivity for simultaneous detection of the three pesticides.

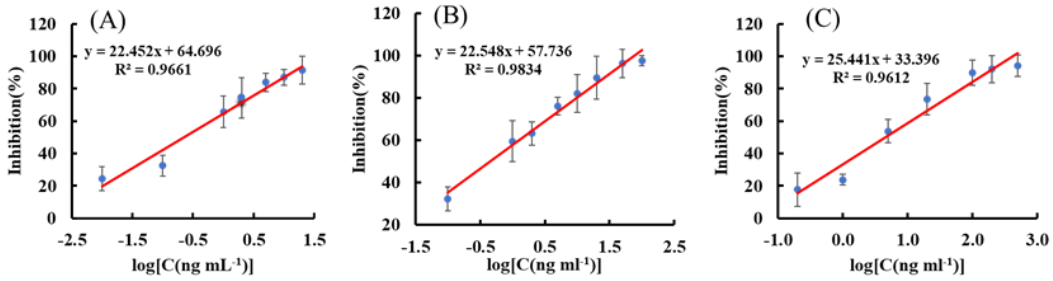

Figure 8. The standard curve of triazophos (A), parathion (B), and chlorpyrifos (C).

Method validation

To validate the accuracy and precision of the developed ddPCR-based bio-barcode immunoassay, apple, cabbage, cucumber, and pear were used for a spike-and-recovery experiment using LC-MS/MS. The spiked recoveries of LC-MS/MS were in

the range of 89.1%-109.8%, with RSDs in between 1.3%-11.4% (Table 3). To further validate the applicability of the established method, the recovery of the proposed method and LC-MS/MS in the pear matrix were compared (Figure 9). The two methods had a good linear relationship with a correlation coefficient (R^2) of 0.9263, 0.9337, and 0.9186. In conclusion, the developed method can be used for simultaneous detection of OPs in various matrices, such as apple, cabbage, pear, and cucumber.

Table 3. Recovery and relative standard deviations (RSDs) of the proposed method and LC-MS/MS.

Pesticides	Sample	Spiked level (μg kg^{-1})	Current method		LC-MS/MS	
			Recoveries (%)	RSD (%)	Recoveries (%)	RSD (%)
Triazophos	Apple	5	78.4	9.32	95.4	2.82
		10	81.2	11.2	103	4.31
		50	92.1	10.3	96.4	7.53
	Cabbage	5	83.2	10.5	98.5	6.13
		10	91.4	14.3	104	3.42
		50	88.3	12.5	97.6	4.52
	Pear	5	93.6	16.4	109	3.38
		10	87.2	11.3	108	1.69
		50	98.9	16.7	91.6	2.70
	Cucumber	5	95.3	15.6	94.3	5.38
		10	90.1	13.4	99.2	8.16
		50	86.7	10.7	89.1	5.98
Parathion	Apple	5	96.4	14.6	93.6	4.54
		10	94.3	12.5	96.5	11.4
		50	90.1	11.5	89.4	2.43
	Cabbage	5	88.7	16.4	95.6	3.59
		10	89.5	15.2	89.7	5.46
		50	90.6	12.1	90.5	8.71
	Pear	5	78.5	14.0	92.6	5.68
		10	87.5	13.6	97.5	3.40
		50	92.7	15.4	109	1.92
	Cucumber	5	98.7	11.3	102	10.2
		10	88.3	13.2	110	8.75
		50	76.9	14.6	90.6	2.52
Chlorpyrifos	Apple	10	76.5	13.7	93.1	9.33
		50	78.4	15.6	96.5	4.24
		100	81.3	11.1	103	7.15
	Cabbage	10	90.2	10.7	107	5.38
		50	89.6	12.4	99.6	1.90
		100	85.3	16.5	90.4	3.68
	Pear	10	91.8	9.7	104	8.89
		50	93.2	10.6	105	1.66
		100	78.8	15.7	89.2	5.44
	Cucumber	10	75.5	14.3	95.6	6.46
		50	87.6	8.3	105	1.31
		100	80.1	14.8	98.3	9.52

404

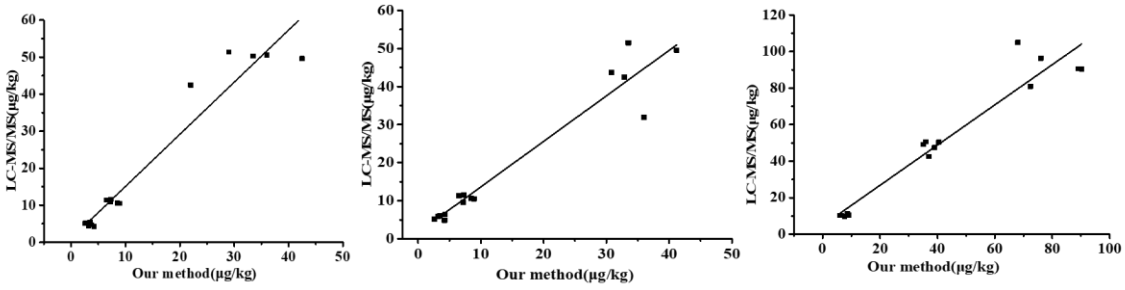

Figure 9. Comparison between the bio-barcode immunoassay-ddPCR and LC-MS/MS in pear sample.

Comparison with bio-barcode immunoassay based on a qPCR

We established a bio-barcode immunoassay based on qPCR and set an intuitive comparison with the proposed method for detecting OPs. The results are shown in Table 4. The values of IC_{50} and IC_{10} for triazophos, parathion, and chlorpyrifos were 1.17, 4.89, and 19.32 ng mL^{-1}; 0.014, 0.170, and 0.269 ng mL^{-1}. qPCR is relatively less sensitive and has a relatively narrow linear range compared to ddPCR. The ddPCR is an absolute quantitative detection technology. That means researchers don't need to rely on the standard curve to read results. Additionally, the results of ddPCR can be read accurately, even if there is a low concentration of the target template. In this way, it can reduce costs and protects precious samples. The annealing temperature, primers, and probes concentration of DNA sequences corresponding to parathion and chlorpyrifos were optimized. The amplification of DNA strand on ddPCR exhibited good suitability at each temperature; however, with the lowest Ct value at 59 °C. Similarly, the smallest Ct value at 57 °C is shown in supplementary materials (Supplementary Figure S1). Ultimately, 58 °C was chosen as the optimal annealing temperature. The concentration of primers and probes at 400 and 200 nmol L^{-1} results

in the highest fluorescence value and the lowest Ct value simultaneously. The optimal primers and probe concentrations were set at 400 and 200 nmol L^{-1}.

Table 4. Assay performance comparison between the ddPCR and the qPCR.

Pesticides	Method	Linear range (ng mL^{-1})	Linear correlation equation	R^2	IC_{50} (ng mL^{-1})	IC_{10} (ng mL^{-1})
Triazophos	ddPCR	0.01–20	y = 22.45x + 64.69	0.9661	0.22	0.004
	qPCR	0.1–20	y = 21.12x + 48.59	0.9631	1.17	0.014
Parathion	ddPCR	0.1–100	y = 22.55x + 57.74	0.9834	0.45	0.007
	qPCR	1–100	y = 27.43x + 31.10	0.9733	4.89	0.170
Chlorpyrifos	ddPCR	0.1–500	y = 25.44x + 33.39	0.9612	4.49	0.121
	qPCR	1–1000	y = 21.55x + 22.29	0.9685	19.32	0.269

Comparison with other immunoassay methods

The method reported here was compared with other immunoassays for detecting OPs in terms of linear range, detection limit, IC_{50}, spiked recovery, and RSD. The results of the lateral flow immunochromatographic assay (LFIC), enzyme-linked immunoassay (ELISA), and biomimetic immunoassay (BI), in addition to our established method, are summarized in Table 5. The main advantage of LFIC is that the test strip is a one-step assay, which can be easily performed on a wide range of

samples, it is suitable for an on-site test, and results are visible to the naked eye. However, the disadvantage is that the sensitivity is not high enough. Molecular imprinting biomimetic immunoassay techniques are widely used due to the high stability of molecular imprinting materials; however, the specificity and the sensitivity need improvement. The digital PCR method showed lower LOD and IC_{50} values than other methods. In other words, it displayed higher sensitivity and applicability to other immunoassay methods for detecting the tested analytes in agricultural products, and its linear range was relatively wide. As an absolute quantitative detection technology, ddPCR was used for the first time to detect pesticides. The results of ddPCR were more accurate, and this method shows good stability in complex matrices. Indeed, the most significant advantage of the developed method is high sensitivity. The developed method would offer remarkable benefits in the face of increasingly strict national standards of pesticides maximum residue limit.

447 **Table 5**. Comparison between the developed method and other immunoassays.

Method	Pesticide	Spiked samples	Type of antibody	Recovery (%)	RSD (%)	Linear range (ng mL^{-1})	LOD (ng mL^{-1})	IC_{50}(ng mL^{-1})	Reference
LFIC[a]	parathion, parathion-methyl, fenitrothion	Cucumber, tomato, orange	monoclonal antibody	67–120	≤19.54	0.98–250	–	3.44, 3.98, 12.49	Zou et al., 2019 [31]
BI[b]	Trichlorfon, chlorpyrifos	Orange, carrot	biomimetic antibody	77.8–92.0	≤4.0	1–100000	18.0, 19.0[f]	11000, 9000	Liu et al., 2018 [32]
ELISA[c]	Paraoxon-ethyl, fenamiphos, triazophos profenofos, acephate,	cabbage, lettuce	polyclonal antibody	85.8–105.5	≤10.4	–	13.0, 24.0, 118, 27.0, 163[g]	354, 527, 2218, 675, 261	Li et al., 2014 [33]
CLEIA[d]	parathion, parathion-methyl, fenitrothion	Apple, Chinese cucumber, rice	monoclonal antibody	73–118	3.35–10.12	0.39–100, 0.10–25, 0.10–25	–	5.43, 1,34, 1.24	Zou et al., 2017 [34]
BCA–ddPCR[e]	Triazophos, parathion, chlorpyrifos	Apple, cucumber, cabbage, pear	monoclonal antibody	75–98	8.3–16.7	0.01–20, 0.1–100, 0.1–500	0.004, 0.007 , 0.121[h]	0.22, 0.45, 4.49	This work

[a] Lateral flow immunochromatographic assay

[b] Biomimetic Immunoassay

[c] Enzyme-Linked Immunoassay

[d] Chemiluminescence enzyme immunoassay

[e] Bio-barcode immunoassay based on ddPCR

[f] IC_{15}

[g] IC_{10}

[h] IC_{10}

In this study, the ddPCR technique was applied to pesticide multi-residue detection, an extension of the bio-barcode immunoassay, and an important innovation in methodological research. Three AuNP probes and MNP probes for triazophos, parathion, and chlorpyrifos were prepared, and three immuno-competitive reaction systems were reacted in the same well. Three sets of primers and probes with reasonable specificity and three specific antibodies ensured the low cross-reactivity of the multi-residue immunoassay. Moreover, compared with bio-barcode immunoassay based on qPCR, it was found that ddPCR combined with bio-barcode immunoassay showed advantages in sensitivity and linear range for the simultaneous detection of three organophosphorus pesticides. This work shows promise for the simultaneous detection of more pesticides and even other small molecule compounds. Overall, the signal amplification technique of bio-barcode combined with the signal re-amplification technique of ddPCR provided the first insights into the multiplex detection of organophosphate pesticides and improved the sensitivity and accuracy of the method.

SUPPORTING INFORMATION

Optimization of annealing temperature, primers, and probe concentrations for parathion and chlorpyrifos.

CORRESPONDING AUTHORS

*E-mail: wangjing05@caas.cn (J. Wang)

jinmaojun@caas.cn (M. J. Jin)

CONFLICTS OF INTEREST

The authors declare no competing financial interest.

ACKNOWLEDGEMENTS

This study was financially supported by the National Key Research Program of China (No. 2019YFC1604503), NIEHS Superfund Research Program (No. P42 ES04699), the Central Public-interest Scientific Institution Basal Research Fund for Chinese Academy of Agricultural Sciences (No. Y2021PT05), and Ningbo Innovation Project for Agro-Products Quality and Safety (No. 2019CXGC007).

REFERENCES

(1) Fantke, P.; Juraske, R. Variability of pesticide dissipation half-lives in plants. Environ Sci Technol. 2004, 47(8), 3548-3562.

(2) Farha, W.; Abd El-Aty, A. M.; Rahman, M. M.; Jeong, J. H.; Shin, H. S.; Wang, J.; Shin, S. S.; Shim, J. H. Analytical approach, dissipation pattern and risk assessment of pesticide residue in green leafy vegetables: A comprehensive review. *Biomed Chromatogr*. **2018**, *32(1)*, 1-18.

(3) Vitola, G.; Mazzei, R.; Poerio, T.; Porzio, E.; Manco, G.; Perrotta, I.; Militano, F.; Giorno, L. Biocatalytic membrane reactor development for organophosphates degradation. *J. Hazard. Mater.* **2019,** *43*, 14048.

(4) Wang, L. L.; Ding, J. J.; Pan, L.; Fu, L.; Tian, J. H.; Cao, D. S.; Jiang, H.; Ding, X. Q. Quantitative structure-toxicity relationship model for acute toxicity of organophosphates via multiple administration routes in rats and mice. *J. Hazard. Mater*. **2021,** *42*, 862–870.

(5) Chen, X. J.; Li, Z. Z.; Guo, J. Y.; Li, D. M.; Gao, H. L.; Wang, Y.; Xu, C. L. Simultaneous screening for marbofloxacin and ofloxacin residues in animal derived foods using an indirect competitive immunoassay. *Food and Agricultural Immunology*. **2017**, *28(3)*, 489–499.

(6) Jiang, H.; Fan, M. T. Multi-analyte immunoassay for pesticides: A review. *Analytical Letters*. **2012**, *45(11)*, 1347–1364.

(7) Li, Y. F.; Sun, Y. M.; Beier, R. C.; Lei, H. T.; Gee, S.; Hammock, B. D.; Xu, Z. L. Immunochemical techniques for multianalyte analysis of chemical residues in food

and the environment: A review. *Trends in Analytical Chemistry*. **2017**, *88*, 25–40.

(8) Qiao, B.; Li, Y. S.; Meng, X. Y.; Sun, Y.; Hu, P.; Lu, S. Y.; Zhou, Y. Development of an indirect competitive ELISA for the detection of acenaphthene and pyrene. *Food and Agricultural Immunology*. **2017**, *28(5)*, 789–800.

(9) Cui, X. Y.; Jin, M. J., Du, P. F.; Chen, G.; Zhang, C.; Zhang, Y. D.; Shao, Y.; Wang, J. Development of immunoassays for multi-residue detection of small molecule compounds. *Food and Agricultural Immunology*. **2018**, *29*, 638-652.

(10) Noh, E.S.; Park, Y.J.; Kim, E.M.; Park, J. Y.; Shim, K. B.; Choi, T. J.; Kim, K. H.; Kang, J. H. Quantitative analysis of Alaska pollock in seafood products by droplet digital PCR. *Food Chem*. **2019**, *275*, 638-643.

(11) Higuchi, R.; Dollinger, G.; Walsh, P. S.; Griffith, R. Simultaneous amplification and detection of specific DNA sequences. *Bio/Technology*. **1992**, *10*, 413-417.

(12) Higuchi, R.; Fockler, C.; Dollinger, G.; Watson, R. Kinetic PCR analysis: real-time monitoring of DNA amplification reactions. *Bio/Technology*. **1993**, *11*, 1026-1030.

(13) Vogelstein, B.; Kinzler, K.W. Digital PCR. *Proc. Natl. Acad. Sci. USA.* **1999**, *96(16)*, 9236-9241.

(14) Liu, Y.; Wang, Y.; Wang, Q.; Zhang, Y. H.; Shen, W. X.; Li, R. H.; Cao, M. J.; Chen, L.; Li, X.; Zou, C. Y.; Zou, Y. Development of a sensitive and reliable reverse transcription droplet digital PCR assay for the detection of citrus yellow vein clearing virus. *Arch Virol*. **2019**, *164(3)*, 691-697.

(15) Zhang, Y. X.; Zhang, Z.; Wang, Z. Y.; Wang, Z. L.; Wang, C. X.; Feng, C. Y.;

Yuan, W. Z.; Lin, X. M.; Wu, S. Q. Development of a droplet digital PCR assay for sensitive detection of porcine circovirus 3. *Mol Cell Probes*. **2019**, *43*, 50-57.

(16) Yang, D.; Hu, T.; Wu, X.; Li, K.; Zhong, Q.; Liu, W. W. Droplet-digital polymerase chain reaction for detection of clinical hepatitis B virus DNA samples. *J Med Virol*. **2018**, *90(12)*, 1868-1874.

(17) Coudray-Meunier, C.; Fraisse, A.; Martin-Latil, S.; Guillier, L.; Delannoy, S.; Fach, P.; Perelle, S. A comparative study of digital RT-PCR and RT-qPCR for quantification of Hepatitis A virus and Norovirus in lettuce and water samples. *International Journal of Food Microbiology*. **2015**, *201(18)*, 17-26.

(18) McMahon, T. C.; Blais, B. W.; Wong, A.; Carrillo, C. D. Multiplexed Single Intact Cell Droplet Digital PCR (MuSIC ddPCR) Method for Specific Detection of Enterohemorrhagic E. coli (EHEC) in Food Enrichment Cultures. *Front Microbiol*. **2017**, *8*, 332.

(19) Wang, M.; Yang, J. J.; Gai, Z. T.; Huo, S. N.; Zhu, J. H.; Li, J.; Wang, R. R.; Xing, S.; Shi, G. S.; Shi, F.; Zhang, L. Comparison between digital PCR and real-time PCR in detection of Salmonella typhimurium in milk. *Int J Food Microbiol*. **2018**, *266*, 251-256.

(20) Singh, G.; Sithebe, A.; Enitan, A. M.; Kumari, S.; Bux, F.; StenstrM, T. A. Comparison of droplet digital PCR and quantitative PCR for the detection of Salmonella and its application for river sediments. *Journal of water and health*. **2017**, *15(4)*, 505-508.

(21) Cremonesi, P.; Cortimiglia, C.; Picozzi, C.; Minozzi, G.; Malvisi, M.; Luini, M.;

553 Castiglioni, B. Development of a Droplet Digital Polymerase Chain Reaction for
554 Rapid and Simultaneous Identification of Common Foodborne Pathogens in Soft
555 Cheese. *Front Microbiol*. **2016**, *7*, 1725.
556 (22) Zhu, P. Y.; Shang, Y.; Tian, W. Y.; Huang, K. L.; Luo, Y. B.; Xu, W. T. Ultra-
557 sensitive and absolute quantitative detection of Cu(2+) based on DNAzyme and
558 digital PCR in water and drink samples. *Food Chem*. **2017**, *221*, 1770-1777.
559 (23) Cheng, N.; Zhu, P. Y.; Xu, Y. C.; Huang, K. L.; Luo, Y. B.; Yang, Z. S.; Xu, W. T.
560 High-sensitivity assay for Hg (II) and Ag (I) ion detection: A new class of droplet
561 digital PCR logic gates for an intelligent DNA calculator. *Biosens Bioelectron*. **2016**,
562 84, 1-6.
563 (24) Cao, C.; Dhumpa, R.; Bang, D. D.; Ghavifekr, Z.; Hogberg, J.; Wolff, A.
564 Detection of avian influenza virus by fluorescent DNA barcode-based immunoassay
565 with sensitivity comparable to PCR. *Analyst*. **2010**, *135(2)*, 337-342.
566 (25) Glowacka K., Kromdijk J., Leonelli L., et al. An evaluation of new and
567 established methods to determine T-DNA copy number and homozygosity in
568 transgenic plants. Plant Cell Environ, 2016, 39(4): 908-917.
569 (26) Glowacka, K.; Kromdijk, J.; Leonelli, L.; Niyogi, K. K.; Clemente, T. E.; Long, S.
570 P. Development and Application of Droplet Digital PCR Tools for the Detection of
571 Transgenes in Pastures and Pasture-Based Products. *Front Plant Sci*. **2018**, *9*, 1923.
572 (27) Wang, X. F.; Tang, T.; Miao, Q. M.; Xie, S. L.; Chen, X. Y.; Tang, J.; Peng, C.;
573 Xu, X. L.; Wei, W.; You, Z. T.; Xu, J. F. Detection of transgenic rice line TT51-1 in
574 processed foods using conventional PCR, real-time PCR, and droplet digital PCR.

575 *Food Control*. **2019**, *98*, 380-388.
576 (28) Cui, X. Y.; Jin, M. J.; Zhang, C.; Du, P. F.; Chen, G.; Qin, G. X.; Jiang, Z. J.;
577 Zhang, Y. D.; Li, M. J.; Liao, Y., Wang, Y. S.; Cao, Z.; Yan, F. Y.; Abd El-Aty, A.
578 M.; Wang, J. Enhancing the Sensitivity of the Bio-barcode Immunoassay for
579 Triazophos Detection Based on Nanoparticles and Droplet Digital Polymerase Chain
580 Reaction. *J. Agric. Food Chem.* **2019**, *67*, 12936−12944.
581 (29) Xu, X.; Ma, X. W.; Zhang, X. J.; Cao, G. J.; Tang, Y. G.; Deng, X.; Kang, Z. H.;
582 Li, M .; Guan, M. Detection of BRAF V600E mutation in fine-needle aspiration fluid
583 of papillary thyroid carcinoma by droplet digital PCR. *Clin Chim Acta*, **2019**, *491*, 91-
584 96.
585 (30) Zhang, C.; Jiang, Z. J.; Jin, M. J.; Du, P. F.; Chen, G.; Cui, X. Y.; Zhang, Y. D.;
586 Qin, G. X.; Yan, F. Y.; Abd El-Aty, A. M.; Hacimuftuoğlug, A.; Wang, J.
587 Fluorescence immunoassay for multiplex detection of organophosphate pesticides in
588 agro-products based on signal amplification of goldnanoparticles and oligonucleotides.
589 *Food Chem.* **2020**, *326*, 126813.
590 (31) Zou, R. B.; Chang, Y. Y.; Zhang, T. Y.; Si, F. F.; Liu, Y.; Zhao, Y.; Liu, Y. H.;
591 Zhang, M. Z.; Yu, X. P.; Qiao, X. S.; Zhu, G. N.; Guo, Y. R. Up-Converting
592 Nanoparticle-Based Immunochromatographic Strip for Multi-Residue Detection of
593 Three Organophosphorus Pesticides in Food. *Front Chem*, **2019**, *7*: 18.
594 (32) Liu Q., Tian J., Jiang M., et al. Direct Competitive Biomimetic Immunoassay
595 Based on Quantum Dot Label for Simultaneous Determination of Two Pesticide
596 Residues in Fruit and Vegetable Samples. Food Analytical Methods, **2018**, *11*: 3015-

3022.

(33) Liu, Q. R.; Tian, J. X.; Jiang, M. D.; Qiao, X. G.; Xu, Z. X. Development of a Broad-Specificity Immunoassay for Determination of Organophosphorus Pesticides Using Dual-Generic Hapten Antigens. *Food Analytical Methods*, **2014**, *8(2)*, 420-427.

(34) Zou, R. B.; Liu, Y.; Wang, S. J.; Zhang, Y.; Guo Y. R.; Zhu G. N. Development and evaluation of chemiluminescence enzyme-linked immunoassay for residue detection of three organophosphorus pesticides. *Chinese Journal of Pesticide Science*. **2017**, *19*, 37-45.

606

For Table of Contents Only

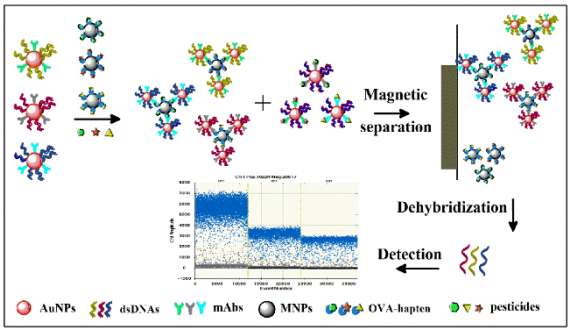

607